Biomedical Optics EXPRESS

Non-invasive respiratory monitoring using long-period fiber grating sensors

M. D. Petrović,[1,*] J. Petrovic,[1] A. Daničić,[1] M. Vukčević,[2] B. Bojović,[1] Lj. Hadžievski,[1] T. Allsop,[3] G. Lloyd,[4] and D. J. Webb[3]

[1]*Vinča Institute of Nuclear Sciences,University of Belgrade, Mike Petrovića Alasa 12-14, 11000 Belgrade, Serbia*
[2]*School of Medicine, University of Belgrade, Dr Subotića 8, 11000 Belgrade, Serbia*
[3]*Aston Institute of Photonic Technologies, Aston Triangle, B4 7ET Birmingham, UK*
[4]*Moog Insensys LTD, Ocean House, Whittle Avenue, Segensworth West, Fareham, P015 5SX, UK*
[*]*marijap@vinca.rs*

Abstract: In non-invasive ventilation, continuous monitoring of respiratory volumes is essential. Here, we present a method for the measurement of respiratory volumes by a single fiber-grating sensor of bending and provide the proof-of-principle by applying a calibration-test measurement procedure on a set of 18 healthy volunteers. Results establish a linear correlation between a change in lung volume and the corresponding change in a local thorax curvature. They also show good sensor accuracy in measurements of tidal and minute respiratory volumes for different types of breathing. The proposed technique does not rely on the air flow through an oronasal mask or the observation of chest movement by a clinician, which distinguishes it from the current clinical practice.

OCIS codes: (060.2370) Fiber optics sensors; (170.3890) Medical optics instrumentation; (170.4580) Optical diagnostics for medicine.

References and links

1. S. Mehta and N. S. Hill, "Noninvasive Ventilation," Am. J. Respir. Crit. Care Med. **163**(2), 540–577 (2001).
2. S. Baudouin, S. Blumenthal, B. Cooper, C. Davidson, A. Davison, M. Elliott, W. Kinnear, R. Paton, and E. Sawicka; British Thoracic Society Standards of Care Committee, "Non-invasive ventilation in acute respiratory failure," Thorax **57**(3), 192–211 (2002).
3. B. J. Semmes, M. J. Tobin, J. V. Snyder, and A. Grenvik, "Subjective and Objective Measurement of Tidal Volume in Critically Ill Patients," Chest **87**(5), 577–579 (1985).
4. M. Folke, L. Cernerud, M. Ekström, and B. Hök, "Critical review of non-invasive respiratory monitoring in medical care," Med. Biol. Eng. Comput. **41**(4), 377–383 (2003).
5. H. Watson, "The technology of respiratory inductance plethysmography," *ISAM Proc. 3rd Intl. Symp. Ambulatory Monitoring*, (Academic, San Diego, Cslig., 1980), p. 537.
6. G. B. Drummond, A. F. Nimmo, and R. A. Elton, "Thoracic impedance used for measuring chest wall movement in postoperative patients," Br. J. Anaesth. **77**(3), 327–332 (1996).
7. C. Davis, A. Mazzolini, and D. Murphy, "A new fibre optic sensor for respiratory monitoring," Australas. Phys. Eng. Sci. Med. **20**(4), 214–219 (1997).
8. A. Aliverti, R. Dellacá, P. Pelosi, D. Chiumello, A. Pedotti, and L. Gattinoni, "Optoelectronic Plethysmography in Intensive Care Patients," Am. J. Respir. Crit. Care Med. **161**(5), 1546–1552 (2000).
9. T. Allsop, K. Carroll, G. Lloyd, D. J. Webb, M. Miller, and I. Bennion, "Application of long-period-grating sensors to respiratory plethysmography," J. Biomed. Opt. **12**(6), 064003 (2007).
10. T. Meier, H. Luepschen, J. Karsten, T. Leibecke, M. Grossherr, H. Gehring, and S. Leonhardt, "Assessment of regional lung recruitment and derecruitment during a PEEP trial based on electrical impedance tomography," Intensive Care Med. **34**(3), 543–550 (2008).
11. K. Konno and J. Mead, "Measurement of the separate volume changes of rib cage and abdomen during breathing," J. Appl. Physiol. **22**(3), 407–422 (1967).
12. J. F. Masa, A. Jiménez, J. Durán, F. Capote, C. Monasterio, M. Mayos, J. Terán, L. Hernández, F. Barbé, A. Maimó, M. Rubio, and J. M. Montserrat, "Alternative Methods of Titrating Continuous Positive Airway Pressure: A Large Multicenter study," Am. J. Respir. Crit. Care Med. **170**(11), 1218–1224 (2004).
13. R. C. C. Barbosa, C. R. Carvalho, and H. T. Moriya, "Respiratory inductive plethysmography: a comparative study between isovolume maneuver calibration and qualitative diagnostic calibration in healthy volunteers assessed in different positions," J. Bras. Pneumol. **38**(2), 194–201 (2012).

#201903 - $15.00 USD Received 25 Nov 2013; revised 18 Jan 2014; accepted 19 Feb 2014; published 12 Mar 2014

14. P. Neumann, J. Zinserling, C. Haase, M. Sydow, and H. Burchardi, "Evaluation of Respiratory Inductive Plethysmography in Controlled Ventilation: Measurement of Tidal Volume and PEEP-Induced Changes of End-expiratory Lung Volume," Chest **113**(2), 443–451 (1998).
15. M. J. Tobin, G. Jenouri, B. Lind, H. Watson, A. Schneider, and M. A. Sackner, "Validation of Respiratory Inductive Plethysmography in Patients with Pulmonary Disease," Chest **83**(4), 615–620 (1983).
16. E. Bar-Yishay, A. Putilov, and S. Einav, "Automated, real-time calibration of the respiratory inductance plethysmograph and its application in newborn infants," Physiol. Meas. **24**(1), 149–163 (2003).
17. P. Blankman and D. Gommers, "Lung monitoring at the bedside in mechanically ventilated patients," Curr. Opin. Crit. Care **18**(3), 261–266 (2012).
18. K. F. Whyte, M. Gugger, G. A. Gould, J. Molloy, P. K. Wraith, and N. J. Douglas, "Accuracy of respiratory inductive plethysmograph in measuring tidal volume during sleep," J. Appl. Physiol. **71**(5), 1866–1871 (1991).
19. N. O. T. Strömberg, "Error analysis of a natural breathing calibration method for respiratory inductive plethysmography," Med. Biol. Eng. Comput. **39**(3), 310–314 (2001).
20. T. Erdogan, "Cladding-mode resonances in short- and long- period fiber grating filters," J. Opt. Soc. Am. A **14**(8), 1760–1773 (1997).
21. R. Kashyap, *Fiber Bragg Gratings* (Academic, 2010).
22. S. W. James and R. P. Tatam, "Optical fibre long-period grating sensors: characteristics and application," Meas. Sci. Technol. **14**(5), R49–R61 (2003).
23. A. Othonos and K. Kalli, *Fibre Bragg gratings:fundamentals and applications in telecommunications and sensing* (Artech House, 1999).
24. L. Zhang, Y. Liu, L. Everall, J. A. R. Williams, and I. Bennion, "Design and realization of long-period grating devices in conventional and high birefringence fibers and their novel applications as fiber-optic load sensors," IEEE J. Quantum Electron. **5**(5), 1373–1378 (1999).
25. M. D. Petrović, A. Daničić, V. Atanasoski, S. Radosavljević, V. Prodanović, N. Miljković, J. Petrović, D. Petrović, B. Bojović, Lj. Hadžievski, T. Allsop, G. Lloyd, and D. J. Webb, "Fibre-grating sensors for the measurement of physiological pulsations," Phys. Scr. T **T157**, 014022 (2013).
26. B. Bojović, M. Vukčević, J. Petrovic, M. D. Petrović, I. Ilić, A. Daničić, T. Allsop, and Lj. Hadžievski, "Apparatus and method for monitoring respiratory volumes and synchroniyation of triggering in mechanical ventilation by measuring the local curvature of the torso surface," Patent Application No. P2012/0373 filed with the IP Office of Serbia.
27. D. G. Altman and J. M. Bland, "Measurement in Medicine: the Analysis of Method Comparison Studies," Statistician **32**(3), 307–317 (1983).
28. T. Allsop, D. J. Webb, and I. Bennion, "Investigations of the spectral sensitivity of Long Period Gratings fabricated in three-layered optical fiber," J. Lightwave Technol. **21**(1), 264–268 (2003).
29. T. Allsop, R. Bhamber, G. Lloyd, M. R. Miller, A. Dixon, D. J. Webb, J. D. Ania Castañón, and I. Bennion, "Respiratory function monitoring using a real-time three-dimensional fiber-optic shaping sensing scheme based upon fiber Bragg gratings," J. Biomed. Opt. **17**(11), 117001 (2012).
30. J. L. Werchowski, M. H. Sanders, J. P. Costantino, F. C. Sciurba, and R. M. Rogers, "Inductance plethysmography measurement of CPAP-induced changes in end-expiratory lung volume," J. Appl. Physiol. **68**(4), 1732–1738 (1990).
31. V. von Tscharner, B. Eskofier, and P. Federolf, "Removal of the electrocardiogram signal from surface EMG recordings using non-linearly scaled wavelets," J. Electromyogr. Kinesiol. **21**(4), 683–688 (2011).
32. J. Iriarte, E. Urrestarazu, M. Valencia, M. Alegre, A. Malanda, C. Viteri, and J. Artieda, "Independent Component Analysis as a Tool to Eliminate Artifacts in EEG: A Quantitative Study," J. Clin. Neurophysiol. **20**(4), 249–257 (2003).

1. Introduction

In medicine, mechanical ventilation is a method to mechanically assist or replace spontaneous breathing. While invasive mechanical ventilation by endotracheal intubation (a tube is inserted through the nose or mouth and advanced into the trachea) is effective in improving alveolar ventilation, it carries risks of traumas during intubation, facilitates infection and may lead to irritation, inflammation and soreness. On the other hand, noninvasive ventilation (NIV) provides the ventilatory support through the patient's upper airway using a mask or mouthpiece. In that manner NIV leaves the upper airways intact, preserves airway defense mechanisms and reduces patient discomfort [1,2].

In NIV, continuous monitoring of respiratory activity is necessary to assess the patient's response to treatment and optimize the ventilator settings. Clinical features that should be assessed are the volume of air moved into or out of the lungs within each breath (tidal volume, V_t) and the volume of air inhaled over time (usually one minute, hence minute volume, V_m). Relying on the air-flow monitoring to follow respiratory volumes may be misleading due to the inevitable air leaks from a mask or mouthpiece. On the other hand, a clinician's observation of the chest wall movement, from which he assesses the lung volume,

#201903 - $15.00 USD Received 25 Nov 2013; revised 18 Jan 2014; accepted 19 Feb 2014; published 12 Mar 2014

is both time consuming and subjective, the decision strongly depending on his experience [1,2]. Tendency to overestimate tidal volume is widespread and is potentially dangerous, especially at low tidal volumes [3].

Therefore, there is a need for non-invasive respiratory monitoring independent of air leaks and this need is well known to the clinical engineering community [4]. As a consequence, a range of new devices detecting thorax and abdomen movements, volume and circumference have been investigated [4–10]. Konno and Mead first demonstrated that respiratory activity during breathing could be measured on the surface of the torso [11]. They have shown that the thoracic and abdominal movements caused by breathing can give a good measure of the volumes of the inhaled air. This discovery has been used to develop several methods and devices: respiratory inductance plethysmography (RIP) [5], transthoracic impedance pneumography [6], fiber-optic respiratory plethysmography [7], optoelectronic plethysmography [8], and plethysmography based on LPG sensors [9]. RIP technology is widely used for the diagnosis of Obstructive Sleep Apnea [12]. However, due to the calibration procedures that either include breathing maneuvers difficult for untrained patients or have poor accuracy [13], high and unpredictable baseline drift [14], and incoherent reports on the accuracy in tidal volume measurements (good [15–17], not consistently precise [14], and poor [18, 19]), it is not used for monitoring during NIV. The use of other abovementioned technologies in lung volume monitoring is still limited to laboratory studies, mainly due to the technical complexity such as the high number of reflective markers (45) in Optoelectronic Plethysmography [8] and LPG sensors (13) in [9].

In an attempt to overcome these limitations, we have developed a new method and apparatus for continuous monitoring of the respiratory tidal volumes based on measurement of thoracic movements. This method is grounded on the hypothesis that the volume of the inhaled air is proportional to the change in a local torso curvature in an area with stiff underlying tissues (bone or cartilage), such as the area of the lower ribs close to the sternum. Technical solution is based on the use of a single fiber-grating sensor and a monochromatic measurement scheme that requires only a photodiode as a detector. The purpose of this study is to test this hypothesis and feasibility of using a single long period grating (LPG) curvature sensor in measuring tidal and minute volumes.

The paper is structured as follows. The working principle of LPG sensors and the particulars of the interrogation scheme are explained in Section 2. The measurement protocol and data analysis method used to check the hypothesis are also described therein. Section 3 shows the results of measurements on a set of 18 healthy volunteers. Advantages and limitations of the proposed method and sensors are discussed in Section 4. Conclusions and directions of future work are given in Section 5.

2. Methods

2.1 LPG curvature sensor

The curvature sensor was based on a long-period fiber grating. The LPG consists of a periodic change in the refractive index profile along the fiber and couples the light from the fundamental core mode to the resonant co-propagating cladding modes that are attenuated as they propagate along the fiber. Coupling to the cladding modes is wavelength selective, resulting in a series of attenuation bends in the transmission spectrum. The resonant wavelength for the v^{th} cladding mode is obtained from the phase matching condition

$$\lambda = \left(n_{co}^{eff} - {}^{v}n_{cl}^{eff} \right) \Lambda \tag{1}$$

where n_{co}^{eff} is the effective index of the core mode, ${}^{v}n_{cl}^{eff}$ the effective index of the v^{th} cladding mode, Λ the period of the grating and λ the resonant wavelength, and is increased with increasing the mode order. The magnitude of an attenuation band depends on the grating length and the mode-coupling strength (hence on the index modulation of the grating and the

#201903 - $15.00 USD Received 25 Nov 2013; revised 18 Jan 2014; accepted 19 Feb 2014; published 12 Mar 2014

overlap between the resonant modes), while its width depends also on the fiber and the grating dispersion [20,21].

The resonant wavelength and the spectral profile of an attenuation band are sensitive to modulations of the fiber guiding properties caused by forces applied to the fiber (strain, bending, load) or changes in local environmental conditions (temperature, refractive index of surrounding material) [22,23]. Change in thorax curvature is sensed as bending of an LPG attached to the thorax. Bending induces strain and stress across the fiber and consequently a change in its refractive index via the strain-optic effect, which manifests as a change in position, shape and amplitude of resonant bands in the transmission spectrum. An alternative solution is to use fiber Bragg gratings (FBGs). However, LPGs have higher sensitivity to bending since the cladding modes generated by an LPG are much more affected by bend-induced refractive index change across the fiber than the back-propagating core modes generated by an FBG. The sensor is evaluated by its accuracy, dynamic measurement range and ease of application.

2.2 Measurement scheme

Bending of the chest wall was measured with an LPG sensor written in a progressive three layered fiber using the point-by-point method [24]. In order to make it compatible with the human body, reduce its cross-sensitivity to environmental conditions and manipulate it easier, the sensor has been encapsulated into a low-temperature curing silicone rubber as described in [9]. The full grating characterization can be obtained by using an optical spectrum analyzer (Fig. 1 inset). However, the high cost of this instrument makes it impractical for clinical use. Here, we employed a simple interrogation module that consists of a fiber-coupled narrowband temperature- and current-stabilized laser diode and a photodiode that measures the power transmitted through an LPG (Fig. 2(a)). We used a DFB laser with a central wavelength 1470.73 nm and a tuning range of 5 nm. The wavelength was changed by changing the DFB laser temperature. For the grating characterization we used a specially designed gauge with three-point bending [25], where the central point of the grating is fixed and the force is applied at the defined distance either side of the center.

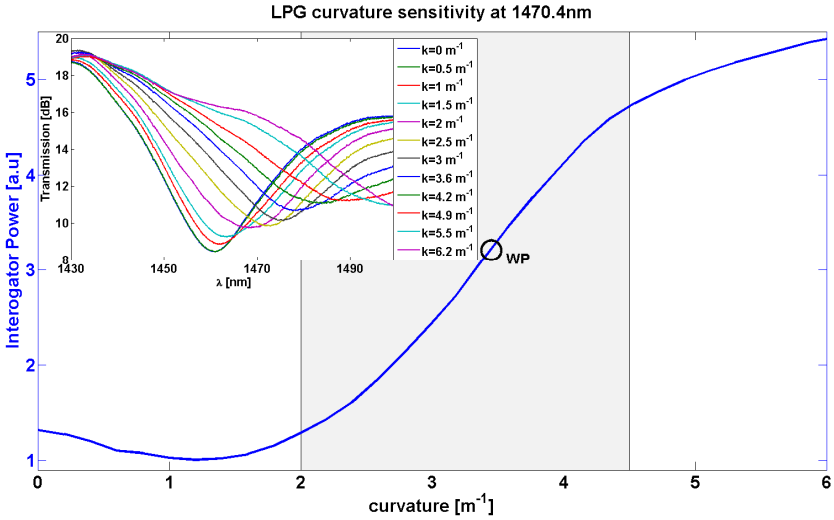

Fig. 1. Power sensitivity of the LPG to bending at 1470.4 nm measured by the interrogator. The working region is shadowed. Inset: Spectral sensitivity of the LPG to bending measured by OSA (Agilent 86142b). During bending the resonance experiences a red shift.

Since we measure the curvature changes around a preset curvature, we want to position the working point (WP) so that the grating characteristic around it is monotonic and, if

#201903 - $15.00 USD Received 25 Nov 2013; revised 18 Jan 2014; accepted 19 Feb 2014; published 12 Mar 2014

possible, linear in the whole breathing range (Fig. 1). To achieve this, we tune the laser into the grating resonance.

During all measurements the volunteers were in the supine position equivalent to the position of patients during mechanical ventilation. A sensor was placed on a surface in the lower third of the thorax in an area with stiff underlying tissues (Fig. 2(b)) and fixed by an elastic bandage that goes around the patient's torso and over the sensor. The right side of the rib cage was chosen in order to reduce the impact of the heart beat on the signal.

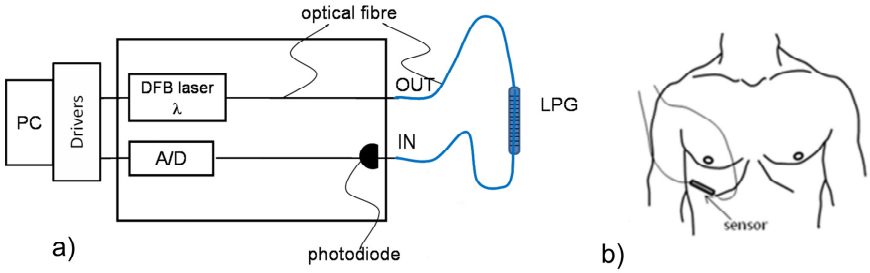

Fig. 2. a) Sensing scheme b) Sensor position on thorax

2.3 Measurement protocol and studied population

The measurement protocol consists of two steps, calibration and test measurements [26].

The curvature signal recorded by the LPG sensor was converted to a volume signal by calibration to the volume simultaneously recorded by a spirometer (SpiroTube, Thor Medical, Budapest).

Although one breathing cycle (breath in and out) is sufficient for calibration, we measured respiratory movements for at least 30 s in order to obtain statistical samples. The calibration was performed during natural breathing with typical tidal volumes of 400 – 800 ml. Volunteers wore nose clips so that air flow was directed only through the spirometer. Test measurements were performed immediately after calibration under the same conditions.

An important part of the volume monitoring in a NIV setting is monitoring of the relative change in minute volume over time with respect to the initial ventilator setting, that is rarely much different from the natural breathing volumes. Additionally, an alarm should be generated when the minute volume is significantly reduced from the initial setting. Hence, for test measurements the volunteers were asked to first breathe naturally and then with a shallow breathing pattern (approximately half the tidal volume of natural breathing).

The study was done on 18 healthy volunteers (9 female and 9 male), aged between 25 and 51 years (33 ± 8 years), and with BMI ranging from 18.4 to 39.2 kg/m^2 (24 ± 5 kg/m^2).

2.4 Data analysis

A LabVIEW program was developed to control the laser diode and perform data acquisition and the raw sensor signal storage. Sampling frequencies of spirometer and sensor signals were 100 Hz and 50 Hz, respectively. They were synchronized, downsampled to 12 Hz (smoothing) and processed off-line by a specially designed MATLAB application.

Since the volume signals from the spirometer and sensor have drifts of different origin (see Fig. 3(a)), we set all end-expiratory volumes and the corresponding minima in both signals to zero (Fig. 3(b)). Zeroing the end of each breath makes a simple and robust solution to drift elimination. Upon the elimination of drift, the calibration function was found by a linear regression of the sensor to the spirometer signal. A calibration function was determined for each volunteer and used in calculation of the respiratory volumes from all test measurements performed on the same volunteer.

#201903 - $15.00 USD Received 25 Nov 2013; revised 18 Jan 2014; accepted 19 Feb 2014; published 12 Mar 2014

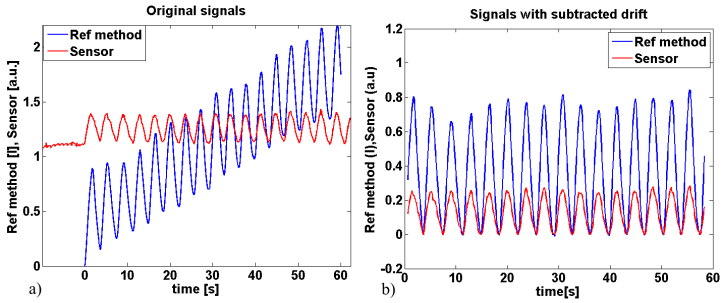

Fig. 3. Examples of a) original signals b) signals with subtracted drift

Each minimum (end-expiratory) value was subtracted from the subsequent maximum (end-inspiratory) value to obtain tidal volumes for both the sensor and spirometer signals. Sum of the tidal volumes over one minute yields the minute volume.

We defined three parameters for the performance metric: uncertainty of the calibration, minute volume error and mean tidal volume error. The uncertainty Δ was defined as a radius of the region around the calibration curve that contains 68% of all measured values. It was normalized to the average tidal volume. The minute volume error was calculated as the relative error of the minute volumes measured by spirometer $V_{\min}^{spiro}$ and sensor $V_{\min}^{sen}$:

$$\text{minute volume error} = \frac{\left|V_{\min}^{spiro} - V_{\min}^{sen}\right|}{V_{\min}^{spiro}}. \qquad (2)$$

The mean tidal volume error was defined as the mean relative error of tidal volumes over a number of respiratory cycles

$$\text{mean tidal volume error} = \frac{1}{N_{cycle}} \sum_{k} \frac{\left|V_{tid,k}^{spiro} - V_{tid,k}^{sen}\right|}{V_{tid,k}^{spiro}}, \quad k = 1 : N_{cycle}, \qquad (3)$$

where $V_{tid,k}^{spiro}$ and $V_{tid,k}^{sen}$ are the tidal volumes in cycle k measured by spirometer and sensor, respectively, and N_{cycle} is the number of respiratory cycles. The purpose of this definition of tidal volume error was to evaluate the discrepancy of tidal volumes of individual breaths, since such discrepancies may be compensated in the calculation of errors in minute volumes.

The paired t tests were used to compare the volumes measured by sensor and spirometer. The level of statistical significance was taken as $p<0.05$. Hereafter, all data are expressed as (mean ± std) where std is standard deviation, unless stated otherwise.

3. Results

A typical set of the calibration and test results is shown in Fig. 4. Scatter plots a) and b) show that the correlation function between the sensor signal and the volume measured by the spirometer is linear. This trend repeats in all subjects. The coefficient of proportionality, i.e. the slope of the regression line in the scatter plot, was patient dependent. The goodness of fit was judged by the uncertainty Δ (Table 1). The calibration uncertainty Δ_{calib} of the whole group was (7.0 ± 2.2) %, with the test uncertainty Δ_{test} (7.8 ± 2.4) % for natural breathing and (11.3 ± 2.8) % for shallow breathing. This proves our hypothesis that a change in respiratory volume is proportional to the change in a local torso curvature.

In the test phase, the volumes measured by a calibrated sensor were compared to the simultaneous recordings of the volumes measured by the spirometer, see Table 1 (e.g. Fig. 4(c) and 4(d)). The minute volume error was (8.7 ± 4.4) % for the natural and (10.1 ± 5.8) % for the shallow breathing. The paired t test did not show statistically significant differences

#201903 - $15.00 USD Received 25 Nov 2013; revised 18 Jan 2014; accepted 19 Feb 2014; published 12 Mar 2014

between the minute volumes measured by the sensor and spirometer for both natural (p = 0.97, t = –0.04)) and shallow breathing (p = 0.42, t = –0.83).

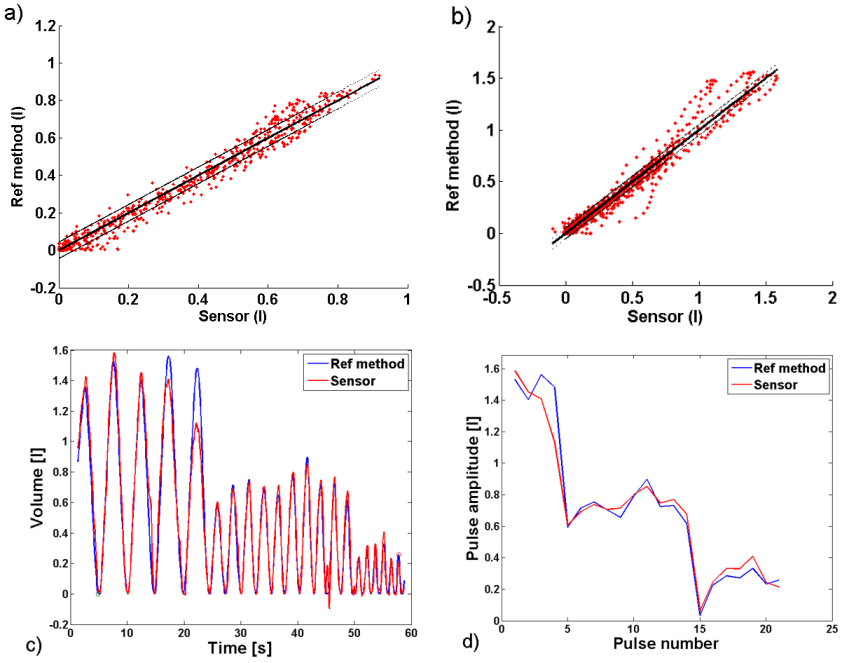

Fig. 4. a), b) Scatter plot (dots) and the calibration function (inner line) and Δ region (outer lines) in calibration and test step, respectively, c) calibrated sensor output, d) tidal volume extracted from c)

Table 1. Test results: sensor vs spirometry*

		minute volume [l]			tidal volume [ml]				
		sensor	Spiro meter	Error [%] Eq. (2)	sensor	Spiro meter	Error [%] Eq. (3)	Δ_{calib} [%]	Δ_{test} [%]
natural breathing	mean	11.0	11.0	8.7	570	570	10.5	7.0	7.8
	std	5.0	4.6	4.4	210	190	3.8	2.2	2.4
shallow breathing	mean	12.0	11.8	10.1	330	320	15.0	7.0	11.3
	std	6.0	5.8	5.8	90	90	4.8	2.2	2.8

* The error columns represent the mean and the standard deviation of the moduli of relative errors for the group. This is different from the mean relative error of the group that is, for example, zero for natural breathing.

Plots in Fig. 4(c) and 4(d) show that the sensor can accurately measure transitions between deep, natural and shallow breathing, which is important for detecting a reduction in minute volume during NIV.

The mean tidal volume error on the whole group was (10.5 ± 3.8) % for the natural and (15.0 ± 4.8) % for the shallow breathing. The identity plot in Fig. 5(a) shows good agreement between the mean tidal volumes measured by the two methods. The Bland-Altman plot in Fig. 5(b) was used as an indicator of potential bias of the tidal volume measurement. Here,

#201903 - $15.00 USD Received 25 Nov 2013; revised 18 Jan 2014; accepted 19 Feb 2014; published 12 Mar 2014

the differences between the tidal volumes obtained by two methods were plotted (with their signs) as a function of the average tidal volume obtained by these methods [27]. The mean of these differences is an indicator of the relative bias towards small/large volumes and their standard deviation is the estimate of error [27]. The obtained bias of (−1.0 ± 9.9) % for natural and (−2.9 ± 11.5) % for shallow breathing is very low and practically insignificant.

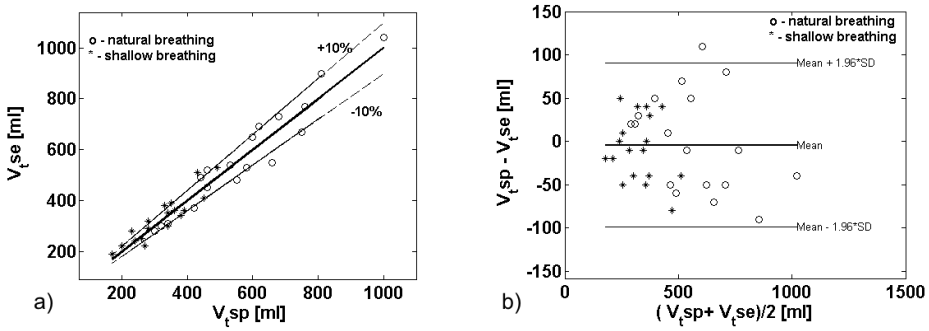

Fig. 5. a) Identity plot of mean V_t recorded by sensors vs. the corresponding values measured by spirometer for each of 18 healthy volunteers for natural breathing (o) and shallow breathing (*). b) Bland-Altman plot of difference in mean V_t measured by the two methods. The middle line represents the mean difference between these two methods (bias) and the outer lines represent 95% limits of agreement (± 1.96 std of bias)

The sensor resolution (the smallest signal that the sensor can detect) achieved by the current LPG interrogation scheme was 0.3 ml. The accuracy of the method is limited by the respiratory signal contamination by the heart beat signal. We have found that by positioning the sensor to the right side of the rib cage, the heart beat signal can be significantly reduced or eliminated. The accuracy of the tidal volume measurement was better than 60 ml. We note that the current interrogation scheme scan rate of 100 Hz allows for simultaneous detection of the cardiac and respiratory signals by the same sensor.

4. Discussion

Due to the out-coupling of light from the core to the radiation cladding modes, LPGs are sensitive to changes in environmental parameters. Therefore, one attenuation band may be simultaneously sensitive to several parameters which makes it impossible to distinguish the contribution of a wanted measurand [22]. The sensor construction was designed to prevent the grating from experiencing changes in the refractive index of the sensor surroundings by using a progressive three-layered fiber whose second cladding served as an isolator [28]. The effect of rapid temperature fluctuations have been reduced by encapsulating the fiber into a low-temperature curing silicone rubber [9], which is also convenient for application on the surface of a human body. Currently, the presented procedure with a sensor attachment by an elastic bandage is sensitive to the upper-body movements, that the subject makes voluntarily or not, that may cause a displacement of the sensor from the initial position and hence, a displacement of the working point. This can lead to two types of signal distortion: saturation on larger curvatures or crossing the turning point on lower curvatures (see Fig. 1), both easily observable in the signal. By changing the laser-diode current, it would be possible to tune the laser wavelength to the optimal working point fast enough to allow for automatic correction of the sensor working point upon the movement of the subject. Furthermore, the sensor movement with respect to the subject can be prevented by application of self-adhesive sensor patches. While these improvements would make measurements operator-independent, the need for calibrating the sensor to some reference method for every subject will remain.

Fiber gratings with linear response can be arranged into 2D sensor networks. This level of complexity is necessary for the measurement of the absolute volumes [9] or torso shape reconstruction [29]. While the grating network is also capable of measuring tidal volumes,

#201903 - $15.00 USD Received 25 Nov 2013; revised 18 Jan 2014; accepted 19 Feb 2014; published 12 Mar 2014

the single-sensor scheme is simpler, easier to implement and less susceptible to signal distortion due to the movements of the soft abdominal tissues.

Compared to RIP, the most commonly used competitive method, our method performs better in two important aspects, accuracy and drift. Firstly, the studies of RIP performed under the same conditions as the study described here, that also use the calibration method not requiring subject cooperation, report the maximum tidal volume error round −24% (Fig. 6 in [30]) (with the mean error of −6.39%) on a set of 7 healthy volunteers [30] and the maximal tidal volume error of 24% on a set of 10 healthy volunteers [19]. The maximum tidal volume error on a set of 18 volunteers reported here was 17% (with the mean error of 0.4%). Secondly, unlike RIP, our method does not suffer from high and unpredictable baseline drift. Although a weak drift in the light source intensity is present, it is much slower than a respiratory cycle and does not introduce errors in tidal and minute volume measurements.

Finally, we note that the heart-beat signal that contaminates the useful signal and thus limits the measurement accuracy can be removed by one of the known signal-separation techniques, such as those applied in the separation of electrocardiographic from electromyographic and electroencephalographic signals [31,32]. On the other hand, the simultaneous detection of the respiratory and cardio signals by a single sensor opens the door to the development of sophisticated multi-parameter monitoring schemes.

5. Conclusion

We have presented and validated a measurement method and optical fiber-grating sensing scheme that permits monitoring of lung volume through a real-time measurement of tidal and minute volumes. The novelty of the proposed method is that it is based on a correlation between the change in local torso curvature and the change in lung volume. In the paper we report on the study that proves this correlation by applying a two-step calibration-test procedure to a series of healthy volunteers and show that it is linear for clinically relevant breathing patterns. The technical novelty of our work lies in facts that we use a single fiber-grating sensor and a monochromatic measurement scheme that requires only a photodiode as a detector. A good agreement of tidal and minute volumes measured simultaneously by sensors and spirometer as a reference, proves sensor accuracy and consistency in time. An LPG was a sensor of choice since it has a greater sensitivity to bending than an FBG. The proposed single-sensor scheme is non-invasive, simple, low-cost and easy to implement. Furthermore, the sensing system can be made compact and easy to implement as a part of the mechanical ventilators but also can be a standalone device, potentially opening up the possibility of long term and ambulatory monitoring and home care applications. Moreover the proposed method can be implemented on both male and female patients with comparable accuracy and the calibration does not require patient cooperation. Importantly, it does not suffer from the flaws of air-flow measurements associated with the leaks from oronasal masks and is also more convenient for patients. The presented LPG sensor completely eliminates the need for chest movement observation by clinicians. These preliminary results are promising and indicate that the method proposed here could be used in NIV. Future work will be directed towards compensation of bodily movements, optimization of the working point, higher-order corrections to the calibration curve and on-line data analysis.

Acknowledgments

We acknowledge support of the Ministry of Education and Science and Technological Development of Serbia (Project III45010).

#201903 - $15.00 USD Received 25 Nov 2013; revised 18 Jan 2014; accepted 19 Feb 2014; published 12 Mar 2014